Available online at www.sciencedirect.com
ScienceDirect
Ceramics International 35 (2009) 997–1002
CERAMICS INTERNATIONAL
www.elsevier.com/locate/ceramint

# Dry sliding wear of zirconia-toughened alumina with different metal oxide additives

Ashis Kumar Dey [a], Koushik Biswas [b,*]

[a] Department of Metallurgy and Materials Engineering, Bengal Engineering and Science University Shibpur, Howrah-711103, India
[b] Department of Metallurgical and Materials Engineering, Indian Institute of Technology, Kharagpur-721302, India

Received 17 January 2008; received in revised form 10 February 2008; accepted 6 April 2008
Available online 10 July 2008

**Abstract**

Tribological behaviour of zirconia-toughened alumina (ZTA) with different metal oxide additives was studied. Solid oxide lubricants ($MO_x$; M = Cu, Ti, Mg, Zn, Mn) were added in small quantities (~8–11 wt%) to provide a self-lubrication action and thereby to decrease the coefficient of dry friction. Dry mixed ceramic composites powders were compacted and pressureless sintered at different temperatures. Densification studies show that near full densities (>97%) were obtained for ZTA ceramic containing both $TiO_2$–CuO and $TiO_2$–$MnO_2$ at 1450 °C. Phase and qualitative compositional analysis was done using X-ray diffraction (XRD) and energy-dispersive spectroscopy (EDS). Tribological behaviour of the various ZTA composites was tested by dry sliding the different specimens against SiC abrasive grit paper at a load of 50 N. The lowest specific wear rate of $9.2 \times 10^{-5}$ $mm^3/N\ m$ and coefficient of friction of 0.35 were observed for the ZTA ceramic composite with $TiO_2$–$MnO_2$. The basic wear mechanisms were abrasion and grain pullout as corroborated from scanning electron microscopy (SEM) images.


*Keywords:* A. Sintering; B. Microstructure; C. Friction; ZTA

## 1. Introduction

Oxide ceramics such as alumina and zirconia are industrially utilized as cutting tools, a variety of bearings, biomaterials, and thermal and corrosion-resistant coatings due to their high hardness, chemical inertness, high melting points, and ability to retain mechanical strength at elevated temperatures [1]. Enhanced fracture toughness of zirconia strengthens the alumina matrix, which is a hard, brittle and low cost ceramic [2,3]. Stress-induced phase transformation toughening and/or stress-induced micro-crack toughening occur in zirconia-toughened alumina (ZTA) by the presence of the monoclinic zirconia resulting in stress around the zirconia particles. These toughening mechanisms are used effectively for increasing fracture toughness, but the wear resistance is reduced as compared to pure alumina [3].

Since last two decades, research on wear behaviour of ceramic materials, particularly on alumina, Y-TZP, ZTA, SiC and $Si_3N_4$, focuses on the material development with little attention on coefficient of friction [2–20]. Influences of different tribological conditions on these ceramics are unique and have specific advantages and disadvantages. As in alumina, when subjected to higher contact load, shows a mild to severe wear behaviour. Similarly, Y-TZP under high sliding velocities, SiC and $Si_3N_4$ in ambient service condition (due to oxidation) suffer severe wear.

To minimize the wear (by fatigue and other mechanisms) and subsequent large energy losses due to friction, the coefficient of friction should be <0.2 for all service conditions [6–9]. However the minimum coefficient of friction obtained in ZTA ceramic is ~0.4 [1,2,8]. Thus, researchers tried to introduce a self-lubricating mechanism in the ceramic composites with low frictional force suitable for application under extreme load and high dry sliding velocity even at elevated temperature under vacuum [1,2,8–10]. In tribological behaviour of ZTA, Trabelsi et al. [11] in their work showed that the addition of zirconia to alumina lowers the wear resistance due to the decrease in hardness. He et al. [12] reported that

* Corresponding author. Tel.: +91 3222 283244/281788; fax: +91 3222 282280.
*E-mail address:* k_biswas@metal.iitkgp.ernet.in (K. Biswas).

0272-8842/$34.00 © 2008 Published by Elsevier Ltd and Techna Group S.r.l.
doi:10.1016/j.ceramint.2008.04.006

under high loading condition, a transition in wear behaviour for ZTA occurs when undoped $ZrO_2$ exceeds a threshold limit of 20 vol%. They suggested a change in wear mechanism from plastic deformation with some grain pullout to a fracture-dominated wear process. Most investigators [12–14] concluded that an optimum amount of zirconia should be in the tune of 10–12 vol% (in ZTA) considering a trade-off between improvements in fracture toughness, decreased grain size and lower hardness.

To improve the wear properties, Kamiya et al. [14] synthesized particulate ($Al_2O_3$ or SiC) reinforced ZTA and reported lowest wear rate when tested under collision (erosive wear test). In a different study, He et al. [12] observed a mild wear with a very low wear rate of $2 \times 10^{-8}$ $mm^3$/N m for ZTA under reciprocal dry sliding (against stainless steel plate) at contact pressure of 300 MPa. Different investigators studied these composites with various types of oxide added in small amounts with the intension of modifying microstructures, improving mechanical properties, chemical stability, etc. However these were not intended for friction reduction [15–19].

Modification of tribological behaviour due to the presence of second phase was first reported by Ravikiran et al. [20] when they studied the influence of interface formed on the pin surface during dry sliding wear of ZTA against steel disc. They observed that wear rates were low at very low and at very high speed due to metal transfer and formation of oxides ($FeAlO_3$ and $Fe_3O_4$) on the pin surface, whereas at intermediate speeds, high wear rate was attributed to the absence of protective layer and increased amount of abrasion. In systematic studies of Kerkwijk et al. [1,2], effect of different soft oxides (such as CuO, $MnO_2$, $B_2O_3$, MgO, ZnO) on alumina and Y-TZP was observed and they found no significant improvement due to the addition of soft oxides except for the ZTA containing CuO. They observed a reduction in coefficient of friction from 0.7 to 0.43 and a specific wear rate of $10^{-7}$ $mm^3$/N m when sliding against alumina balls. In a similar study by Pasaribu et al. [19], addition of copper oxide to alumina and zirconia (3Y-TZP) ceramics showed a significant contribution in reducing friction when tested at various humidity levels and at elevated temperatures. The coefficient of friction of alumina doped with 5 wt% CuO sliding against alumina had showed a reduction of friction from 0.55 to 0.4 at 23 °C and 40% relative humidity. Possible formation of relatively soft compound-like $CuAlO_2$ and enhancement of super-plastic deformation behaviour by addition of CuO may lead to improved tribological behaviour [1,2,19]. However, alumina and zirconia doped with 5 wt% CuO showed high coefficient of friction (~0.6 to 1) when tested at elevated temperatures (100–500 °C).

Bearing these in mind, the present study focuses on tribological behaviour of ZTA composites with various combinations of soft oxides in small quantities without significant degradation of mechanical properties. The SEM, XRD, EDS analyses are done in order to elucidate structure–properties relationship.

## 2. Experimental

### 2.1. Materials and synthesis

The starting powders used to fabricate green bodies were commercially available $Al_2O_3$, $ZrO_2$, MgO, ZnO, $TiO_2$, CuO and $MnO_2$ powders. The characteristics of these powders are given in Table 1. Compositional variations were done by adding two different oxide powders (4 wt% each) from ZnO, $TiO_2$, CuO and $MnO_2$ powders to the mixture of $Al_2O_3$–$ZrO_2$–MgO. The powder specifications and denominations are detailed in Table 2.

Specific quantities of different powders were dry mixed in a rotary mill for 24 h. The different powder premixes were then pressed at 400 MPa pressure to disc-shaped specimen (Ø25.9 mm).

Sintering was carried out in a high-temperature PID-controlled muffle furnace (Naskar made, India) at different temperatures for 1 h in air. The heating rate was 15 °C/min from room temperature to 1200 °C and thereafter 10 °C/min to the sintering temperature.

### 2.2. Characterization of ceramics

The density of the sintered pellets was measured by Archimedes' water displacement principle:

$$\rho_s = \frac{m_s \rho_w}{m_s - m_w} \quad (1)$$

where $\rho_s$ and $\rho_w$ are the sintered and water densities, respectively, and $m_s$ and $m_w$ are the mass of the sintered pellet and mass of the pellets in the water, respectively. The relative density ($\rho_{rel}$) was calculated by dividing the sintered density $\rho_s$ by the theoretical density ($\rho_{th}$) calculated from the rule of mixtures.

X-ray diffractometry (XRD) was performed in Philips X-ray diffractometer (PW 1840, Holland) using filtered Mo Kα

Table 1
Characteristic of starting ceramic powder

| Powder | Manufacturer | Chemical analysis (wt%) | Density (gm/cc) |
|---|---|---|---|
| $Al_2O_3$ | Loba Chemie, Mumbai, India | Purity 99.1% | 3.97 |
| $ZrO_2$ | Loba Chemie, Mumbai, India | Purity 97%; $SiO_2$ 0.25, $TiO_2$ 0.16, $Fe_2O_3$ 0.07 | 5.68 |
| MgO | Loba Chemie, Mumbai, India | Pb 0.002, Fe 0.1, sulphate 0.05, chloride 0.1 | 3.60 |
| ZnO | Loba Chemie, Mumbai, India | Purity 99%; chloride 0.005, sulphate 0.02, Pb 0.005, Fe 0.001 | 5.60 |
| $TiO_2$ | Loba Chemie, Mumbai, India | Purity 99%; sulphate 0.05, Pb 0.003, Fe 0.005 | 4.23 |
| CuO | Loba Chemie, Mumbai, India | Purity 97%; chloride 0.1, sulphate 0.06, Fe 0.1 | 6.31 |
| $MnO_2$ | Merck Limited, Mumbai, India | Purity >70% | 5.10 |

Table 2
Specifications of the starting powders

| Powder denomination | $Al_2O_3$ (wt%) | $ZrO_2$ (wt%) | MgO (wt%) | Additive oxides (wt%) |
|---|---|---|---|---|
| ZTA-1 | 77.6 | 19.4 | 3 | – |
| ZTA-2 | 71.4 | 17.85 | 2.75 | $MnO_2$ 4, ZnO 4 |
| ZTA-3 | 71.4 | 17.85 | 2.75 | $MnO_2$ 4, CuO 4 |
| ZTA-4 | 71.4 | 17.85 | 2.75 | ZnO 4, CuO 4 |
| ZTA-5 | 71.4 | 17.85 | 2.75 | $TiO_2$ 4, $MnO_2$ 4 |
| ZTA-6 | 71.4 | 17.85 | 2.75 | $TiO_2$ 4, CuO 4 |

radiation with a wavelength of $\lambda = 0.70930$ Å on sintered samples. Qualitative phase analysis is accomplished by comparison with JCPDS standards.

Microstructures of the sintered and worn specimens were observed by optical (Leica, Germany) and scanning electron microscope (Zeiss Supra 40 attached with Oxford energy-dispersive X-ray microanalysis). The polished specimens (1 μm surface finish) were thermally etched at 1200 °C for 2 h in air. Thermally etched, worn-out and fractured specimens were sputtered with gold to avoid charging effect under SEM.

### 2.3. Sample preparation and tribological conditions

To study tribological behaviour, different ZTA ceramics discs with a diameter of 25.4 mm were polished to 1 μm surface finish and cleaned ultrasonically in ethanol for 30 min. Dry sliding wear friction tests were performed by sliding the specimens over SiC abrasive grit paper (size ~3 μm) applying a constant load of 50 N. The stroke of the reciprocating motion was 25 cm. During the wear test of each sample, SiC grit paper was replaced by new one after a sliding distance of 50 m. The maximum sliding distance was 1.8 km. The coefficient of friction ($f$) was measured by the ratio of the measured shear force to the applied normal force.

## 3. Results and discussion

### 3.1. Sintering, microstructure and phase evolution

The average sintered densities of all ZTA composites are reported in Table 3. Sintered densities of ZTA specimens with $TiO_2$–CuO and $TiO_2$–$MnO_2$ oxides are relatively higher (>97% of the theoretical density) than other compositions. Fig. 1 shows the effect of sintering temperature on the final densities of all ZTA ceramics. It is noted that except for the above two compositions, all the sintered specimens show a decrease in sintered density with increase in sintering temperature. This may be attributed to simultaneous presence of volatile oxides (such as ZnO, $MnO_2$ and CuO) with high vapour pressure. On the contrary, in ZTA with $TiO_2$–CuO, there is formation of (and most probably in $TiO_2$–$MnO_2$) an eutectic (at 16.7 wt% $TiO_2$) in $TiO_2$–CuO phase diagram [21], which may cause formation of liquid phase (small) that results in higher densified sintered bodies. The presence of solidified liquid structure (shown in Fig. 2) was found in the specimen of ZTA-6. Formation of $Cu_3TiO_4$, $MnTiO_3$ and presence of other phases such as α-$Al_2O_3$, m-/t-$ZrO_2$, α-$MnO_2$ are confirmed by XRD analysis (shown in Fig. 3). However formation of $Al_2TiO_5$ was not observed in presence of CuO or $MnO_2$ as it facilitates the formation of $(Zr,Ti)_xO_4$-type of phases [22]. Unlike CuO, $MnO_2$ forms a solid solution with $Al_2O_3$ [17] and hence a peak shift corresponding to alumina was observed in XRD patterns between these two compositions.

In macroscopic scale, the observed SEM micrograph (Fig. 4(a)) reveals a distribution of zirconia-rich phase. (EDS result shows concentration (by weight) of Zr 39.5%, Al 4%, Ti 5%, Mn 1.8%, Mg 3.7%, O 47%) (white grains) and alumina grains (dark gray).) Microstructure of fractured specimen shows (Fig. 4(b)) faceted grains with average size between 2 and 3 μm. Both CuO and $MnO_2$ lead to grain coarsening either by enhancing liquid phase diffusion (CuO) or by forming solid solution ($MnO_2$) [17]. The addition of $TiO_2$ also acts as grain

Table 3
Relative densities of all ZTA composites sintered at different temperatures

| Powder denomination | Theoretical density (gm/cc) | Relative density (%) | | |
|---|---|---|---|---|
| | | 1300 °C | 1450 °C | 1600 °C |
| ZTA-1 | 4.29 | – | – | 91 |
| ZTA-2 | 4.37 | 92.5 | 87.0 | 83 |
| ZTA-3 | 4.40 | 92.5 | 90.5 | 87 |
| ZTA-4 | 4.35 | 96.0 | 93.4 | 81 |
| ZTA-5 | 4.37 | 95.2 | 99.5 | 91 |
| ZTA-6 | 4.32 | 95.6 | 97.5 | 91 |

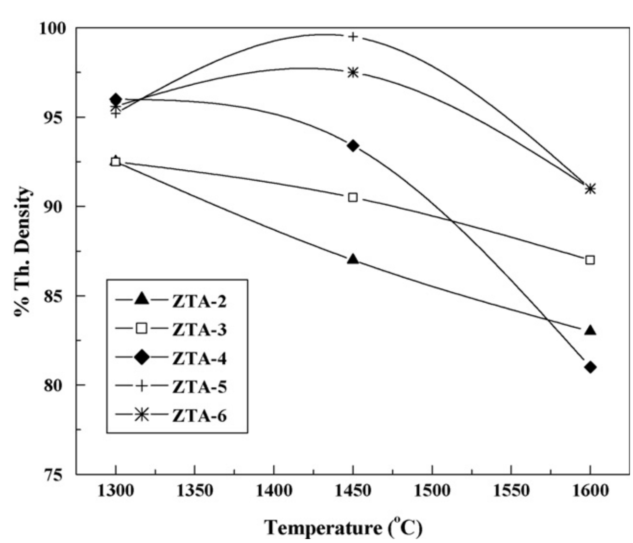


Fig. 1. Sintered density variation of different ZTA composites with temperatures.

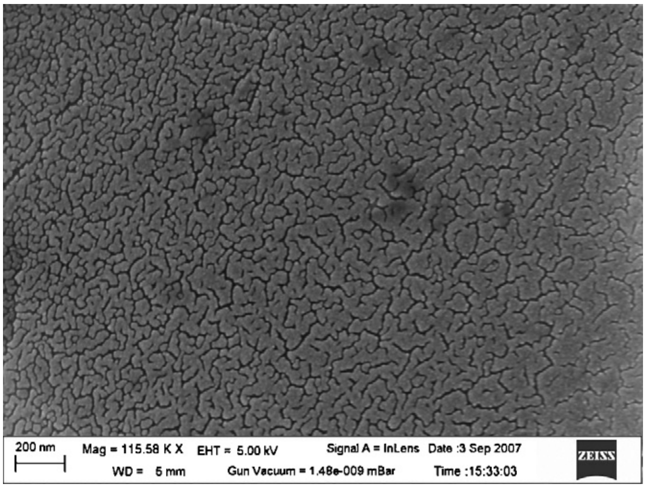


Fig. 2. HR-SEM image of ZTA-6 sintered at 1450 °C showing presence of solidified liquid phase (dendritic) structure at the grain-boundary region.

coarsener. It enters $Al_2O_3$ substitutionally ($Ti^{4+}$ replaces $Al^{3+}$) there-by increasing concentration of aluminium-ion vacancies which enhances the aluminium-ion diffusion by a vacancy mechanism [17]. In order to retard grain-growth, addition of 3 wt% MgO was mandatory as conventional grain-growth inhibitor [17].

Observing densification and microstructural behaviour, it can be concluded that $TiO_2$ contributes significantly to densification of the composites and the maximum density was obtained at 1450 °C.

### 3.2. Tribological behaviour

Dry sliding wear tests were performed on different specimens and the results obtained are shown in Fig. 5. From the plot of wear volume vs. sliding distance, it is clear that except for ZTA-2, all other ZTA composites show moderate to low wear rates. The lowest specific wear rate of $9.2 \times 10^{-5}$ $mm^3$/N m is observed for ZTA-5 when tested against SiC grit paper at a load of 50 N. Under same tribological conditions, higher specific wear rates (more than a factor of 4) are obtained for ZTA-6 and ZTA-3. Wear rate of ZTA-2 seems linear with sliding distances and hence is very high.

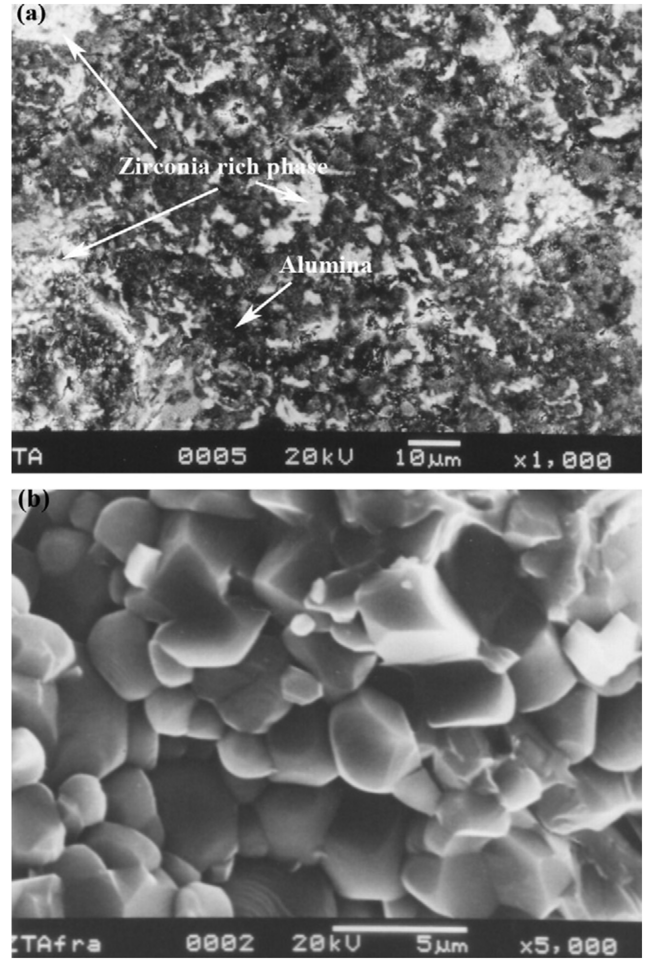


Fig. 4. SEM micrographs of (a) polished and thermally etched and (b) fractured ZTA-5 sample.

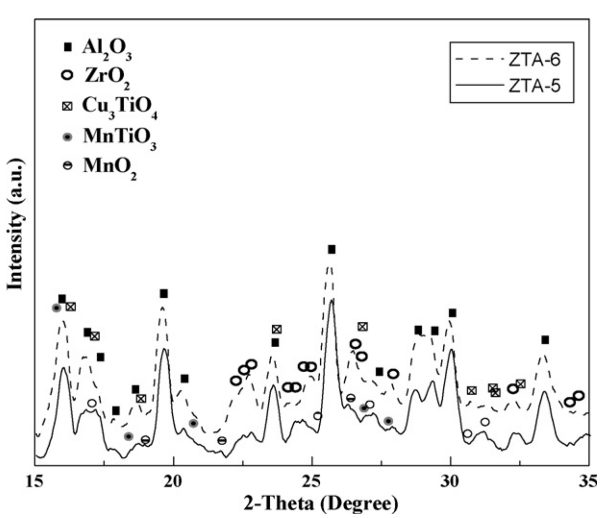


Fig. 3. X-ray diffraction patterns for ZTA-5 and ZTA-6 showing evolution of different phases during sintering at 1450 °C.

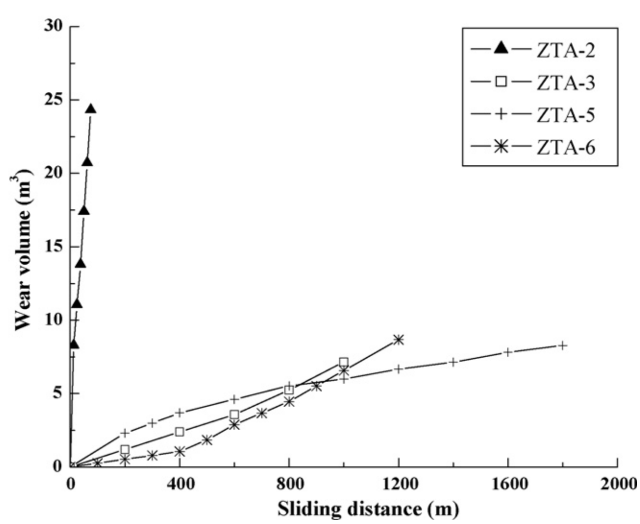


Fig. 5. Dry sliding wear behaviour of different ZTA composites under 50 N load at a constant sliding speed of 0.5 m/s.

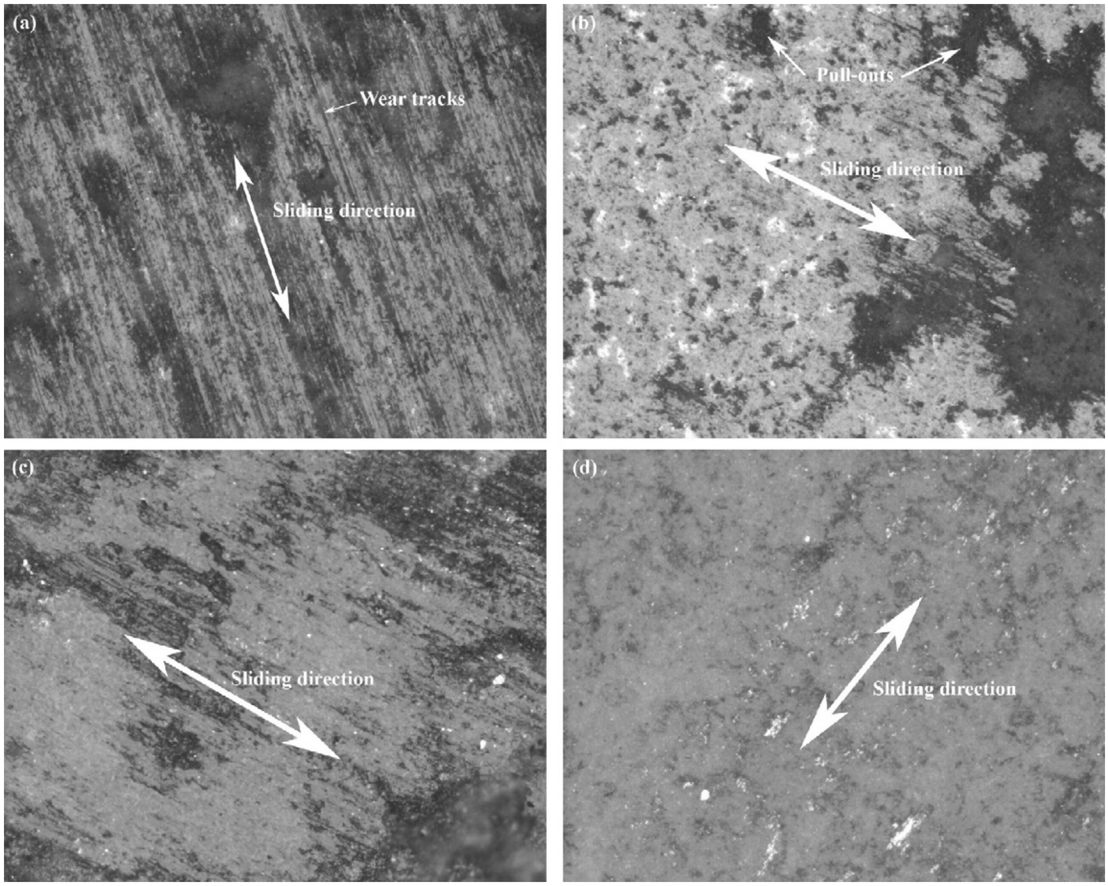


Fig. 6. Optical micrographs of worn-out surfaces of different ZTA composites showing wear tracks: (a) ZTA-2, (b) ZTA-3, (c) ZTA-5 and (d) ZTA-6 (magnification 200×).

Examination of the worn surfaces of the disc-shaped specimens gives an indication for the wear mechanisms occurred. For ZTA-2 ceramics, a relatively rough surface is observed in Fig. 6(a). This causes a higher contact pressure (as number of contact asperities are low) causing larger tangential stress behind the trailing edge and hence more wear loss by grain pullouts and fragmentations. On contrary, a mixture of rough and relatively large smooth regions is observed in case of ZTA-3, -5 and -6 (Fig. 6(b)–(d)). The presence of CuO-rich grain-boundary phases (for ZTA-3 and ZTA-6) and formation of $Al_2O_3$–$MnO_2$ solid solution (for ZTA-3 and ZTA-5) enhance the wear resistance. Although grain-boundary phases have very little influence on wear mechanism in case of fine-grained structure, however, in brittle fracture (such as grain pullout), the role of grain-boundary phase plays predominant role [4]. Formation of rather softer phase increases the contact area which in-turn reduces the frictional contact stresses. This reduces the tendency of fracture wear and hence low wear loss [4]. Earlier works by Kerkwijk et al. [1,2] were unable to explain the role of CuO or $MnO_2$ clearly and reported probable presence of a softer phase. In case of ZTA composites containing CuO, it is observed that friction (wear volume) gradually increases with sliding distances. This occurs due to the release of second phase as well as presence of CuO which enhances the super-plastic deformation [1,2]. On the other hand, specimen containing $MnO_2$ forms a solid solution with alumina matrix and increases the hardness which decreases the wear rate with increase in sliding distance [17]. EDS analyses of the wear track and debris on ZTA-5 show the presence of $MnO_2$ and alumina. This is also in well agreement with the reported literature [1,2]. As opposed to Evans and Marshall's [23] postulation (wear rate is inversely proportion to power of hardness), the wear rate here decreases with increase of sliding

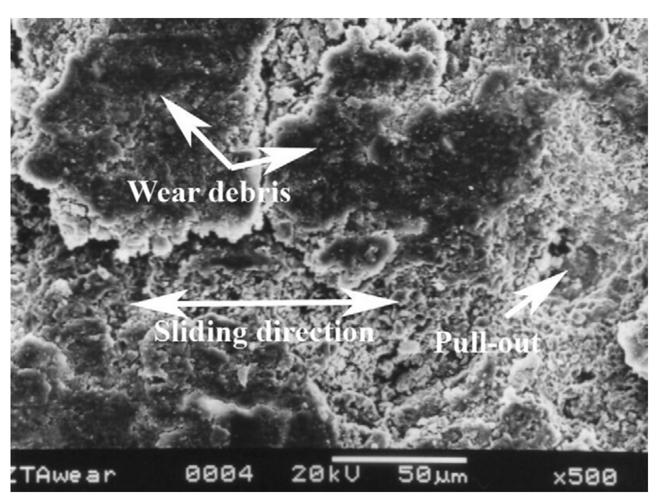


Fig. 7. SEM image revealing smeared wear debris formed during dry sliding wear of ZTA-5.

distance as the wear debris formed are compacted and smeared to the worn surfaces for which more polished surface is obtained. This may also result higher frictional area, lower contact stresses and hence in a lowest specific wear rate is obtained with a lowest coefficient of friction among all the composites. SEM micrographs (Fig. 7) of ZTA-5 specimen for the wear surface confirms the presence of smeared surface with some grain pullouts as possible mechanism of wear.

### 3.3. Coefficient of friction

The lowest value of coefficient of static friction ($\mu$ = 0.35) is obtained for ZTA-5 and the highest value of coefficient of static friction ($\mu$ = 0.7) is obtained for ZTA-2 after the wear test. The value of coefficient of static friction for other two composites (ZTA-6 and ZTA-3) is calculated to be 0.4. Thus from the results obtained, it is evident that ZTA-5, which contains $TiO_2$ and $MnO_2$, shows a very low wear rate and also a low value of coefficient of static friction among all the composites of different composition.

## 4. Conclusions

Additions of CuO, $MnO_2$ and $TiO_2$ enhance the sintering kinetics of ZTA composites and it is possible to densify this ceramic even at lower temperature $\leq$1450 °C by pressureless sintering. Microstructural and phase evolution during sintering and wear tests plays a significant role in densification and controlling of the wear rate, wear mechanism and coefficient of friction. The dry sliding wear tests of different ZTA composites reveal that addition of $TiO_2$ and $MnO_2$ (4 wt% each) to ZTA helps to achieve low specific wear rate with low coefficient of friction. The main wear mechanisms in these cases are grain pullout and removal of secondary phases.

## References


[1] B. Kerkwijk, M. Garcia, W.E. Van Zyl, L. Winnubst, E.J. Mulder, D.J. Sehipper, H. Verweij, Friction behaviour of solid oxide lubricants as second phase in (-alumina and stabilized $ZrO_2$ composites, Wear 256 (2004) 182–189.

[2] B. Kerkwijk, A.J.A. Winnubst, H. Verweij, E.J. Mulder, H.S.C. Metselaar, D.J. Schipper, Tribological properties of nanoscale alumina–zirconia composites, Wear 225–229 (1999) 1293–1302.

[3] J.F. Bartolome, C. Pecharroman, J.S. Moya, A. Martin, J.Y. Pastor, J. Llorca, Percolative mechanism of sliding wear in alumina/zirconia composites, Journal of the European Ceramic Society 26 (2006) 2619–2625.

[4] Y.J. He, A.J.A. Winnubst, A.J. Burggraaf, H. Verweij, P.G.T. van der Varst, G. de With, Sliding wear of $ZrO_2$–$Al_2O_3$ composite ceramics, Journal of the European Ceramic Society 17 (1997) 1371–1380.

[5] K.H. Zum Gahr, W. Bundschuh, B. Zimmerlin, Effect of grain size on friction and sliding wear of oxide ceramics, Wear 162–164 (1993) 269–279.

[6] M. Baumann, K.H. Zum Gahr, Schmierstoffe für keramische Reibpaare: Einfluss von Schichtgitterzwischenstoffen amndt Beispiel von $Al_2O_3$ – Gleitpaarungen, Tribologie und Schmierungs Technik 43 (1996) 23–31 (in German).

[7] M. Woydt, Werkstoffkonzepte fur den Trockenlauf, Tribologie und Schmierungs Technik 44 (1997) 14–19 (in German).

[8] H. Czichos, D. Klaffke, E. Santner, M. Woydt, Advances in tribology: the materials point of view, Wear 190 (1995) 155–161.

[9] K. Adachi, K. Kato, N. Chen, Wear map of ceramics, Wear 203–204 (1997) 291–301.

[10] Y.J. He, A.J.A. Winnubst, D.J. Schipper, P.M.V. Bakker, A.J. Burggraff, H. Verweij, Friction and wear behaviour of ceramic-hardened steel couples under reciprocating sliding motion, Wear 184 (1995) 33–43.

[11] R. Trabelsi, D. Treheux, G. Orange, G. Fantozzi, P. Homerin, F. Thevenot, Relationship between the mechanical properties and wear resistance of alumina zirconia ceramic composites, Tribological Transaction 32 (1) (1989) 77–84.

[12] C. He, Y.S. Wang, J.S. Wallace, S.M. Hsu, Effect of microstructure on the wear transition of zirconia-toughened alumina, Wear 162–164 (1993) 314–321.

[13] K.J. Konsztowicz, R. Langlois, Effects of hetero-flocculation of powders on mechanical properties of zirconia–alumina composites, Journal of Materials Science 31 (1996) 1633–1641.

[14] H. Kamiya, M. Sakakibara, Y. Sakuri, G. Jimbo, S. Wada, Erosion wear properties of tetragonal $ZrO_2$-,$Y_2O_3$-toughened $Al_2O_3$ composites, Journal of the American Ceramic Society 77 (3) (1994) 666–672.

[15] J.R. Seidensticker, M.J. Mayo, Superplasticity in 3Y TZP doped with small amounts of copper oxide, Scripta Metallurgica et Materialia 31 (12) (1994) 1749–1754.

[16] C.M.J. Hwang, I.-W. Chen, Effect of a liquid phase on the superplasticity of 2 mol% $Y_2O_3$ stabilized tetragonal zirconia polycrystals, Journal of the American Ceramic Society 73 (6) (1990) 1626–1632.

[17] H. Erkalfa, Z. Misirli, T. Baykara, The effect of $TiO_2$ and $MnO_2$ on densification and micro-structural development of alumina, Ceramic International 24 (2) (1998) 81–90.

[18] C.A. Batman, S.J. Bennison, M.P. Harmer, Mechanism for the role of magnesia in the sintering of alumina containing small amounts of a liquid phase, Journal of the American Ceramic Society 72 (7) (1989) 1241–1244.

[19] H.R. Pasaribu, K.M. Reuver, D.J. Schipper, S. Ran, K.W. Wiratha, A.J.A. Winnubst, D.H.A. Blank, Environmental effects on friction and wear of dry sliding zirconia and alumina ceramics doped with copper oxide, International Journal of Refractory Metals and Hard Materials 23 (2005) 386–390.

[20] A. Ravikiran, G.R. Subbanna, B.N. Pramila Bai, Effect of interface layers formed during dry sliding of zirconia toughened alumina (ZTA) and monolithic alumina against steel, Wear 192 (1996) 56–65.

[21] F.-H. Lu, F.-X. Fang, Y.-S. Chen, Eutectic reaction between copper oxide and titanium dioxide, Journal of the European Ceramic Society 21 (2001) 1093–1099.

[22] T. Ulrike, E. David, The $ZrO_2$–$TiO_2$ phase diagram, Journal of Materials Science 40 (17) (2005) 4571–4577.

[23] A.G. Evans, D.B. Marshall, Wear mechanisms in ceramics, in: D.A. Rigney (Ed.), Fundamentals of Friction and Wear of Materials, ASM International, 1981, pp. 439–453.